

Enhanced acceleration in a self-modulated-laser wake-field accelerator

J. Krall, A. Ting, E. Esarey, and P. Sprangle

Beam Physics Branch, Plasma Physics Division, Naval Research Laboratory, Washington, DC 20375-5346

(Received 6 April 1993)

An alternative configuration of the laser wake-field accelerator is proposed in which enhanced acceleration is achieved via resonant self-modulation of the laser pulse. This requires laser power in excess of the critical power for relativistic guiding and a plasma wavelength short compared to the laser pulse length. Relativistic and density wake effects strongly modulate the laser pulse at the plasma wavelength, resonantly exciting the plasma wave and leading to enhanced acceleration.

PACS number(s): 29.17.+w, 52.40.Nk, 41.75.-i

I. INTRODUCTION

Plasma-based accelerators are being widely researched as candidates for the next generation of particle accelerators [1]. One promising concept is the laser wake-field accelerator (LWFA) [2-4], in which a short ($\tau_L < 1$ ps), high-power ($P > 10^{12}$ W) laser pulse propagates in plasma to generate a large-amplitude ($E > 1$ GV/m) wake field, which can trap and accelerate a trailing electron bunch. In the standard LWFA, efficient wake generation requires $L \simeq \lambda_p/2$, where L is the full-width-at-half-maximum length of the laser intensity profile on axis, $\lambda_p = 2\pi c/\omega_p$ is the plasma wavelength, $\omega_p = (4\pi n_0 e^2/m)^{1/2}$, and n_0 is the ambient plasma density. In this case, the peak axial electric field is given by [2-4] $E_z \simeq (\pi^2 m c^2/e) a_0^2 / (4\lambda_p \gamma_\perp)$, where $\gamma_\perp = (1 + a_0^2/2)^{1/2}$ and $a_0 = e A_0/mc^2$ is the normalized amplitude of the laser vector potential field [5], which is assumed to be linearly polarized throughout this paper. To improve the final energies of accelerated particles in the LWFA, higher accelerating fields and longer interaction distances are required. Accelerating fields can be increased by reducing the plasma wavelength and hence the laser pulse length, which is limited by technological considerations. Longer interaction distances may be achieved if the laser pulse can be optically guided [3-4, 6-8].

In this paper, we propose a self-modulated LWFA in which enhanced acceleration is achieved via resonant self-modulation of the laser pulse. This occurs when (a) the laser pulse extends axially over several plasma wavelengths, $L > \lambda_p$, and (b) the peak laser power satisfies $P \geq P_c \simeq 17(\lambda_p/\lambda_0)^2$ GW, where P_c is the critical power [6] for relativistic optical guiding and λ_0 is the laser wavelength. At fixed laser parameters, both conditions can be met by choosing a sufficiently high plasma density. Operation in the self-modulated regime could have a dramatic impact on LWFA experiments now being planned in the United States and elsewhere.

II. SELF-MODULATION OF THE LASER PULSE

We have found that in the self-modulated regime, enhanced wake fields are generated, i.e., accelerating fields are more than an order of magnitude greater than

those generated by a laser pulse with $L \simeq \lambda_p/2$, assuming fixed laser parameters. Acceleration is enhanced for four reasons. First, since a higher density is required (assuming L fixed), the wake field will be increased: $E_z \sim n_0^{1/2}$. Second, the resonant mechanism excites a very-high-amplitude wake field in comparison to the standard LWFA. Third, since $P > P_c$, relativistic focusing further enhances the laser intensity, increasing a_0 . Fourth, simulations show that a portion of the pulse will remain guided over multiple laser diffraction lengths, extending the acceleration distance.

The mechanism can be understood by considering a long laser pulse $L \gg \lambda_p$, with power $P \simeq P_c$, such that the body of the pulse is relativistically guided [3]. The finite rise time of the pulse will create a low-amplitude wake field within the laser pulse. Alternatively, this plasma wave can be generated via a forward-Raman-scattering (FRS) instability, as was suggested by Tajima and Dawson [2]. In the wake field, each region of decreased density acts as a local plasma channel to enhance the relativistic focusing effect, while each region of increased density causes defocusing [7,8]. This results in a low-amplitude modulation of the laser pulse at λ_p . The modulated laser pulse resonantly excites the wake field and the process continues in an unstable manner. This instability, which is observed to develop on a time scale associated with laser diffraction, resembles a highly nonlinear two-dimensional form of the usual FRS instability. It is distinguished from FRS by its two-dimensional nature and by its growth rate, which increases dramatically as the $P \geq P_c$ threshold is crossed.

In the standard LWFA, the acceleration distance is limited by the diffraction length, or Rayleigh length, of the laser pulse: $Z_R = (k_0/2)r_0^2$, where $k_0 = 2\pi/\lambda_0$ and r_0 is the radius of the laser waist. At the high plasma densities and extended laser propagation lengths associated with the self-modulated LWFA, single-stage acceleration can be limited by detuning due to the reduced group velocity v_g of the laser pulse, rather than by diffraction. Here $v_g \simeq c[1 - (\lambda_0/\lambda_p \gamma_\perp)^2/2]$, where $L \gg \lambda_p$ has been assumed [4]. One-dimensional theory indicates that phase detuning limits the maximum acceleration to $\Delta\gamma_{\max} \simeq \pi\lambda_p^2 a_0^2 \gamma_\perp / (2\lambda_0^2)$, assuming fixed a_0 and $\lambda_p a_0^2/\lambda_0 \gg 1$. With current laser technology [9], acceleration of electrons to ~ 100 MeV appears possible us-

ing a single-stage, standard LWFA [10,11]. We find, however, that resonant self-modulation and relativistic guiding can enhance considerably the acceleration in the self-modulated LWFA. We will illustrate this via two numerical simulations. The first is a standard case which is optimized in the usual sense, with $L = \lambda_p/2$. The second is a self-modulated case, in which the plasma density is increased such that $L > \lambda_p$ and $P > P_c$ are achieved (all other parameters remain unchanged).

III. MODEL EQUATIONS

These simulations were based on the laser-plasma fluid model described in Refs [8,11], which utilizes $(r, \xi = z - ct, \tau = t)$ coordinates. The laser pulse moves in the positive z direction such that the front of the laser pulse remains near $\xi = 0$. The physical region of interest extends from $\xi = 0$, where the plasma is unperturbed, to $\xi < 0$. The model is valid when $Z_R \gg L$, $Z_R \gg \lambda_p$, $\lambda_0 \ll r_0$, and $\lambda_0 \ll \lambda_p$. Laser-pulse evolution is described by the wave equation

$$\left[\nabla_{\perp}^2 + \frac{2ik_0}{c} \frac{\partial}{\partial \tau} + \frac{2}{c} \frac{\partial^2}{\partial \tau \partial \xi} \right] \hat{\mathbf{a}}_f = k_p^2 \rho_s \hat{\mathbf{a}}_f. \quad (1)$$

To include phase detuning effects, the $\partial^2/\partial \tau \partial \xi$ term is retained in Eq. (1), in contrast to Refs. [8,11]. In Eq. (1), $\hat{\mathbf{a}}_f$ is the slowly varying amplitude of the normalized vector potential of the laser pulse [$\mathbf{a}_f = \hat{\mathbf{a}}_f \exp(ik_0 \xi)/2 + \text{c.c.}$, where c.c. denotes complex conjugate], $k_p = \omega_p/c$, $\rho_s = n_s/\gamma_s n_0$, n_s is the slowly varying component of the plasma density and γ_s is the slowly varying component of the relativistic factor of the plasma. The plasma response to a given laser field $\hat{\mathbf{a}}_f$ is given by [8]

$$\nabla_{\perp}^2 \mathbf{a}_s = k_p^2 \rho_s \mathbf{u}_s - \frac{\partial(\nabla \phi_s)}{\partial \xi}, \quad (2a)$$

$$\left[\nabla_{\perp}^2 + \frac{\partial^2}{\partial \xi^2} \right] \phi_s = k_p^2 [\gamma_s \rho_s - \rho^{(0)}], \quad (2b)$$

$$\frac{\partial(\mathbf{u}_s - \mathbf{a}_s)}{\partial \xi} = \nabla(\gamma_s - \phi_s), \quad (2c)$$

and

$$\gamma_s = 1 + (\mathbf{u}_{\perp s}^2 + \hat{\mathbf{a}}_f \cdot \hat{\mathbf{a}}_f^* / 2 + \psi_s^2) / [2(1 + \psi_s)], \quad (2d)$$

where the Coulomb gauge has been used ($\nabla \cdot \mathbf{a}_s = 0$) and $\psi_s \equiv \phi_s - a_{z,s}$. In Eqs. (2a)–(2d), $\mathbf{a}_s = e \mathbf{A}_s / mc^2$ and $\phi_s = e \Phi_s / mc^2$ are the normalized vector and scalar potentials, respectively, $\mathbf{u}_s = \mathbf{p}_s / mc$ is the normalized momentum, $\rho^{(0)} = \rho_s(\xi = 0)$, the subscript s denotes the slowly varying component, and the plasma ions are assumed to be immobile. In the axisymmetric case, Eqs. (2a)–(2d), along with $\nabla \cdot \mathbf{a}_s = 0$, can be combined to yield a single equation for ψ_s in terms of $|\hat{\mathbf{a}}_f|^2$, which is solved numerically [8,11]. This model neglects certain laser-plasma instabilities [12–14]. In particular, Raman side scattering could limit the effective longitudinal extent of a laser pulse with $P > P_c$ [14]. This will be discussed further at the end of Sec. V.

IV. SIMULATION RESULTS

In these runs, we will consider a Gaussian laser pulse with $\lambda_0 = 1 \mu\text{m}$, $a_0 = 0.70$, $r_0 = 31 \mu\text{m}$ and $L = 45 \mu\text{m}$ (150 fs), such that $Z_R = 0.3 \text{ cm}$. Here we define a_0 to be the amplitude of the laser vector potential \mathbf{a}_f at the point of minimum focus in vacuum. In this case, the peak laser power is $P = 21.5(a_0 r_0 / \lambda_0)^2 \text{ GW} = 10 \text{ TW}$ and the energy per pulse is 1.5 J, well within the bounds of present technology [9]. The simulation geometry is illustrated in Fig. 1. We begin at $\tau = 0$ with the laser pulse outside the plasma. The plasma density is “ramped up” to reach full density at $c\tau = 2Z_R$. The laser pulse is initially converging such that in vacuum it would focus to a minimum spot size of $r_0 = 31 \mu\text{m}$ at $c\tau = 3Z_R$. The simulation continues until $c\tau = 10Z_R = 3.0 \text{ cm}$.

According to standard LWFA theory [2,3], the optimum wake field will be obtained at a plasma density for which $\lambda_p \approx 2L = 90 \mu\text{m}$, or $n_0 = 1.4 \times 10^{17} \text{ cm}^{-3}$. At this density, $P < P_c \approx 140 \text{ TW}$ such that relativistic guiding effects are unimportant. In fact, the presence of the plasma has little effect on the evolution of the laser pulse, which reaches a peak normalized intensity of $|\hat{\mathbf{a}}_f|^2 = 0.56$ at $c\tau = 3Z_R$ (in this run, the laser spot size versus time closely tracks the line for vacuum diffraction shown in Fig. 1). This is further illustrated in Fig. 2 (dashed line), where the peak accelerating field, plotted versus time, is symmetric about $c\tau = 3Z_R$.

To study the acceleration and trapping of electrons by the wake field, a particle code is used to accelerate a distribution of 30000 noninteracting test particles in the time-resolved electric and magnetic wake fields of the simulation. Here we consider a continuous electron beam with initial energy of 3.0 MeV and normalized emittance $\epsilon_n = 130 \text{ mm mrad}$. The beam is initially converging such that in vacuum it would focus to a minimum rms radius $r_b = 200 \mu\text{m}$ at $c\tau = 3Z_R$. After $c\tau = 10Z_R = 3.0 \text{ cm}$, a small fraction (0.1%) of the original particle

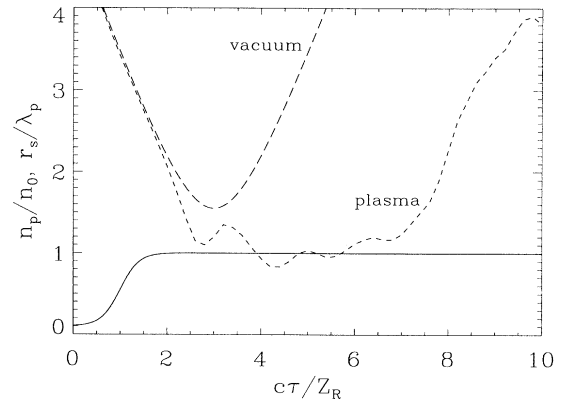


FIG. 1. Ambient plasma density n_p/n_0 vs time (solid line) and spot size r_s/λ_p of the leading laser beamlet plotted vs time for the $n_0 = 2.8 \times 10^{18} \text{ cm}^{-3}$ case. The laser is initially converging such that the minimum spot size in vacuum is reached at $c\tau = 3Z_R$. Here, r_s is defined as the radius enclosing 86.5% of the laser power (for a Gaussian pulse, $a \sim e^{-r^2/2r_s^2}$).

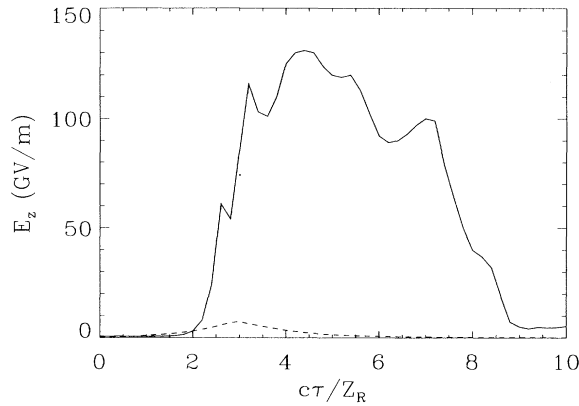


FIG. 2. Peak accelerating field vs time for the $n_0 = 1.4 \times 10^{17} \text{ cm}^{-3}$ case (dashed line) and the $n_0 = 2.8 \times 10^{18} \text{ cm}^{-3}$ case (solid line).

distribution has been trapped and accelerated (simulations show that this fraction can be increased by using a lower emittance beam). At $c\tau = 3 \text{ cm}$, the peak particle energy is 48 MeV (see Fig. 3, dashed line).

We now consider a self-modulated LWFA simulation with parameters nearly identical to those considered above. Here the plasma density has been increased to $n_0 = 2.8 \times 10^{18} \text{ cm}^{-3}$ ($\lambda_p = 20 \mu\text{m}$). This reduces the critical power to $P_c = 6.8 \text{ TW}$, such that $P \approx 1.5P_c$. As the laser parameters have not been changed, the laser pulse now extends over several λ_p .

Three important physical effects come into play in this case. First, because $P > P_c$ and $L > \lambda_p$, resonant self-modulation of the laser pulse will excite a very-high-amplitude wake field. Second, portions of the long laser pulse with $P \geq P_c$ will remain optically guided and focused over multiple Z_R , increasing the acceleration length and enhancing the laser intensity. Third, $\Delta\gamma_{\text{max}} \approx 340$ (170 MeV). However, we will see below that self-focusing enhances the laser intensity by a large factor

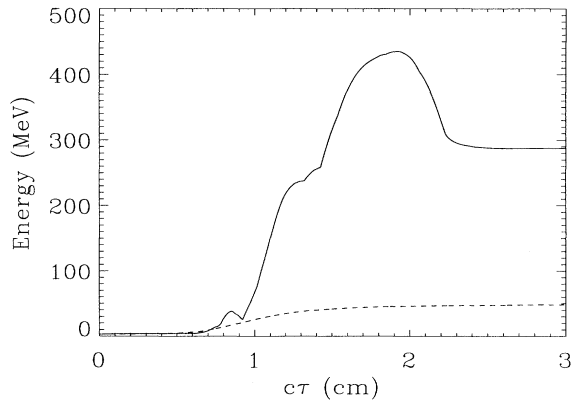


FIG. 3. Peak particle energy vs time for the $n_0 = 1.4 \times 10^{17} \text{ cm}^{-3}$ case (dashed line) and the $n_0 = 2.8 \times 10^{18} \text{ cm}^{-3}$ case (solid line).

(> 10) such that much higher electron energies can be obtained.

Figure 4 shows the normalized laser intensity at (a) $c\tau = 2Z_R$ (just as the laser enters the full-density plasma) and (b) $c\tau = 3.2Z_R$ (just beyond the vacuum focal point). The axial electric field and plasma electron density at $c\tau = 3.2Z_R$ are shown in Figs. 5 and 6, respectively. The laser pulse has been modulated [three peaks are observable in Fig. 4(b), separated by $\approx \lambda_p$] and the plasma wave is highly nonlinear. In addition, relativistic and density wake effects have focused the laser to a much higher intensity than was observed in the previous simulation. Figure 1, which shows the spot size r_s vs time for the leading portion of the laser pulse, indicates that the laser pulse is optically guided over $5.5Z_R$. A plot of the peak accelerating field versus time, Fig. 2 (solid line) further illustrates this point. Here the leading laser “beamlet” initiates a density wake which, when combined with the relativistic focusing effect, results in strong focusing of each of the laser beamlets. Note that the leading portion of the beamlet structure, with length $< \lambda_p / (2\gamma_{\perp})$, diffractively erodes [3,8]. However, the extreme focusing of the laser pulse increases γ_{\perp} such that the erosion is minimized. As a result, the leading beamlet remains focused over multiple diffraction lengths (see Fig. 1). In addition, the group velocity within the modulated pulse varies locally with laser intensity and electron density, further distorting the pulse profile. The laser beamlets continue to distort and erode until $c\tau \approx 7Z_R$, at which time the laser pulse disintegrates entirely. Note also that

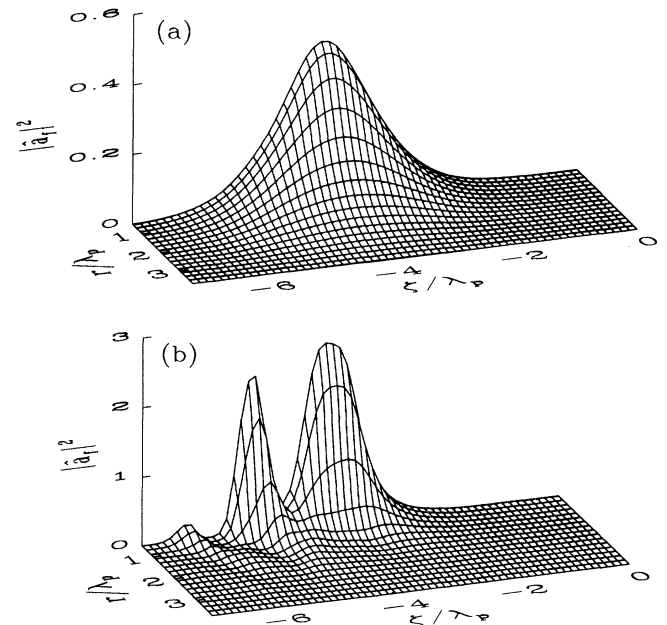


FIG. 4. Laser intensity $|a_f|^2$, sampled over a coarse grid (the numerical grid is much finer), at (a) $c\tau = 2Z_R$ and (b) $c\tau = 3.2Z_R$. The laser pulse is moving towards the right.

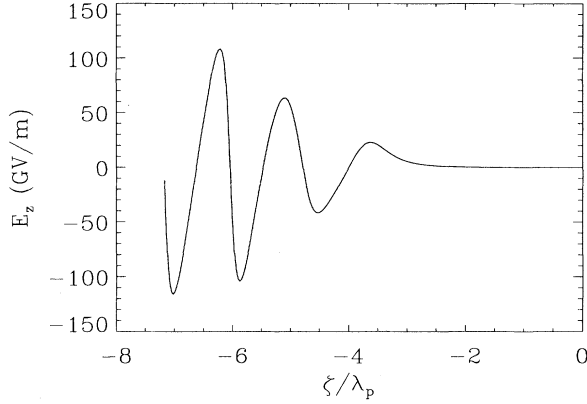


FIG. 5. Axial electric field E_z vs ξ plotted at $c\tau = 3.2Z_R$.

the exponential growth distance of the instability is significantly less than Z_R (the laser enters the plasma at $c\tau = 2Z_R$ and is fully modulated at $c\tau = 3.2Z_R$).

Figure 2 (solid line) also shows that as the pulse becomes fully modulated, the amplitude of the peak accelerating field saturates. We have performed further simulations that suggest an additional saturation mechanism. We find that as the wake amplitude increases to the point that the plasma electrons are expelled entirely from the axis of the simulation, the growth of the instability slows. Our model, however, contains a mathematical singularity at zero plasma-electron density. This is unfortunate for two reasons: first, we were not able to explore this saturation mechanism in detail; second, it has recently been pointed out [15] that in the limit of zero plasma-electron density in the wake, the resulting bare ion channel has favorable (i.e., linear) focusing properties, which tend to preserve the emittance of an accelerated electron bunch. In addition to the two saturation mechanisms discussed above, we have observed that the growth of the instability may be inhibited in some cases. Specifically, the two-dimensional nature of the instability requires that regions of focusing and defocusing occur within the pulse. When defocusing is inhibited, the

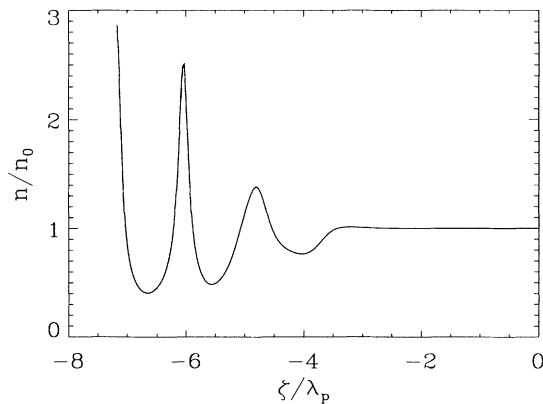


FIG. 6. Plasma-electron density on axis n/n_0 vs ξ plotted at $c\tau = 3.2Z_R$.

growth of the instability can be slowed or stopped entirely. We have observed this in cases where the pulse is converging and is several Rayleigh lengths from focus (here the instability can be suppressed until minimum spot size is reached), and in cases with $P \geq P_c$ in which a density channel is present (this can be either a preformed plasma channel or a plasma-electron channel due to self-channeling). In the case of self-channeling, radial ponderomotive forces expel a large fraction of the plasma electrons from the axis. A sufficiently strong density channel ($\Delta n/n_0 \sim 0.5$) provides additional guiding and can reduce the growth rate of the instability (typically by a factor of 2–3).

As before, a beam of 30 000 noninteracting test particles is injected into the time-resolved wake field, with approximately 2% of the particles being trapped and accelerated (as in the previous case, we find that this fraction can be increased by using a lower emittance beam). The peak particle energy of 430 MeV is observed at $c\tau = 1.8 \text{ cm} = 6Z_R$. At $c\tau = 3.0 \text{ cm} = 10Z_R$, however, the peak particle energy has dropped to 290 MeV due to the reduced group velocity of the laser pulse, which causes the electrons to slip out of phase with the wake field and become decelerated. Figure 3 (solid line) shows acceleration to 430 MeV.

V. COMPARISON TO THE FORWARD RAMAN-SCATTERING INSTABILITY

Finally, we have performed additional simulations to investigate the nature of the highly nonlinear instability observed here. In the broad-pulse regime, $r_0 \gg \lambda_p$, with $P < P_c$, the nonlinear modulation instability described above reduces to the standard FRS instability. In this regime, $a_0 \ll 1$, it is straightforward to analyze the stability of Eqs. (1) and (2) following the approach of Ref. [14]. Consider laser perturbations propagating in the forward direction ($k_\perp = 0$) of the form $\delta a_\pm = \delta \hat{a}_\pm \exp(i(\theta_0 \pm \theta_\pm) + \text{c.c.})$, where $\theta_0 = k_0 z - \omega_0 t$, $\theta_+ = kz - \omega t$, $\theta_- = \theta_+^*$, and the frequency and wave number of the pump laser are related by $\omega_0^2 - c^2 k_0^2 = \omega_p^2(1 - |\hat{a}_f|^2/4)$. The frequency and wave number k of the perturbation satisfy the dispersion relation [14,16] $D(\omega, k) = 0$, where

$$D = (k^2 - k_p^2)(k^2 \delta \omega^2 - k_0^2 \delta \bar{\omega}^2) - k_p^4 a_0^2 c k \delta \omega / 4, \quad (3)$$

$\delta \omega = \omega - ck$ and $\delta \bar{\omega} = \omega - v_g k$ is the frequency in the group-velocity coordinate system ($\xi_g = z - v_g t$, $\tau = t$).

For a semi-infinite beam that exists in the region $\xi_g \leq 0$, the asymptotic behavior of the instability can be determined using a conventional stability analysis [14,17]. This is obtained by solving the equations $D(\delta \bar{\omega}, k) = 0$ and $d[D(\delta \bar{\omega}', k)]/dk = 0$, where $\delta \bar{\omega}' = \delta \bar{\omega} - vk$ and $v \equiv \xi_g / \tau \leq 0$. We have solved Eq. (3) in various limits. For example, in the limit that $(\omega_p / \omega_0)^5 / a_0^2 < |v| < (\omega_p / \omega_0)^2 / a_0^2$ and $a_0 (\omega_p / \omega_0)^2 / (2\sqrt{2}) < |v|$, the behavior of the perturbation is given by $|\delta a_\pm| \sim \exp(\Gamma \tau)$, where

$$\Gamma = \frac{\sqrt{3}}{2} a_0^{2/3} \left(\frac{\omega_p}{\omega_0} \right)^{4/3} \omega_p \left(\frac{|\xi_g|}{c\tau} \right)^{1/3}. \quad (4)$$

Growth rates obtained via simulation were in good agreement with Eq. (4); the scaling with respect to a_0 , ω_p , and ω_0 was confirmed to within 10% (we used $r_L \geq 50\lambda_p$, $\lambda_p = 10\text{--}30\ \mu\text{m}$ and $a_0 = 0.004\text{--}0.10$). Simulations show, however, that the growth of the nonlinear modulation instability greatly exceeds that of the standard FRS instability for cases in which $P \geq P_c$ and the exponential growth time of the FRS instability is long compared to Z_R/c or for cases in which $P \gg P_c$.

Raman side scattering could limit the length of long pulses, $L \gg \lambda_p$, by causing the tail of the pulse to erode [14]. In our simulations, side-scattering radiation with $k_\perp \simeq k_0$ is not resolved due to the finite radial grid size (the grid resolves $\lambda_p \geq 20\lambda_0$). Reference [14], however, estimates that pulses which are not too long, $k_p L \simeq 10\text{--}20$, should be stable to side scatter. The self-modulated case simulated here satisfies this condition. In addition, the results of Ref. [14] describe the linear stability of a uniform laser pulse. As the pulse self-modulates (with an exponential growth length $\ll Z_R$) the two processes will compete. It is possible that, once the laser pulse is fully modulated, it will be stable to side scatter, since a perturbation may not grow significantly within a beamlet of length $< \lambda_p$.

VI. CONCLUSIONS

We have proposed an alternative configuration of the LWFA in which enhanced acceleration (by a factor > 10)

is achieved via resonant self-modulation of the laser pulse (this concept is also discussed in Ref. [18], which was only recently brought to our attention). The self-modulation mechanism requires $P \geq P_c$ and $L > \lambda_p$ (the usual requirement that $L \simeq \lambda_p/2$ is removed). We have demonstrated via simulation the dramatic advantages of the self-modulated LWFA relative to the standard LWFA [1–3]. We have further demonstrated the feasibility of the self-modulated case by confining our simulations to currently available laser and plasma parameters. We should point out that similar improvements over the standard LWFA can be obtained through the use of laser guiding via a performed plasma channel or via pulse tailoring [8,11]. The point of this paper, however, is that a significant enhancement in LWFA performance can be obtained without addressing the technical difficulties that are associated each of these alternatives. It is a notable aspect of these simulations that, by increasing only the plasma density, one can test both the simple linear theory and the highly nonlinear, self-modulation regime described here.

ACKNOWLEDGMENTS

The authors would like to thank G. Joyce (Naval Research Laboratory) and G. Mourou and D. Umstadter (University of Michigan) for enlightening discussions. This work was supported by the Department of Energy and the Office of Naval Research.

-
- [1] See, e.g., *Advanced Accelerator Concepts*, edited by J. Wurtele, AIP Conf. Proc. No. 279 (AIP, New York, 1993).
 - [2] T. Tajima and J. M. Dawson, Phys. Rev. Lett. **43**, 267 (1979); L. M. Gorbunov and V. I. Kirsanov, Zh. Eksp. Teor. Fiz. **93**, 509 (1987) [Sov. Phys. JETP **66**, 290 (1987)]; P. Sprangle, E. Esarey, A. Ting, and G. Joyce, Appl. Phys. Lett. **53**, 2146 (1988); E. Esarey, A. Ting, P. Sprangle, and G. Joyce, Comments Plasma Phys. Controlled Fusion **12**, 191 (1989).
 - [3] A. Ting, E. Esarey, and P. Sprangle, Phys. Fluids B **2**, 1390 (1990); P. Sprangle, E. Esarey, and A. Ting, Phys. Rev. Lett. **64**, 2011 (1990); Phys. Rev. A **41**, 4463 (1990).
 - [4] P. Sprangle and E. Esarey, Phys. Fluids B **4**, 2241 (1992).
 - [5] In terms of the intensity I_0 and the laser wavelength λ_0 , $a_0 \simeq 8.5 \times 10^{-10} [\lambda_0(\mu\text{m})][I_0^{1/2}(\text{W}/\text{cm}^2)]$ for a Gaussian laser pulse.
 - [6] C. E. Max, J. Arons, and A. B. Langdon, Phys. Rev. Lett. **33**, 209 (1974); G. Z. Sun *et al.*, Phys. Fluids **30**, 526 (1987); P. Sprangle, C. M. Tang, and E. Esarey, IEEE Trans Plasma Sci. **PS-15**, 145 (1987); E. Esarey, A. Ting, and P. Sprangle, Appl. Phys. Lett. **53**, 1266 (1988); W. B. Mori *et al.*, Phys. Rev. Lett. **60**, 1298 (1988); A. B. Borisov *et al.*, *ibid.*, **68**, 2309 (1992).
 - [7] E. Esarey and A. Ting, Phys. Rev. Lett. **65**, 1961 (1990).
 - [8] P. Sprangle, E. Esarey, J. Krall, and G. Joyce, Phys. Rev. Lett. **69**, 2200 (1992).
 - [9] G. Mourou and D. Umstadter, Phys. Fluids B **4**, 2315 (1992); J. P. Wateau *et al.*, *ibid.* **4**, 2217 (1992).
 - [10] J. Krall, A. Ting, P. Sprangle, E. Esarey, and G. Joyce, in *Advanced Accelerator Concepts* (Ref. [1]), p. 514.
 - [11] P. Sprangle, E. Esarey, J. Krall, G. Joyce, and A. Ting, in *Advanced Accelerator Concepts* (Ref. [1]), p. 490; J. Krall, G. Joyce, P. Sprangle, and E. Esarey, *ibid.*, p. 528.
 - [12] P. Sprangle and E. Esarey, Phys. Rev. Lett. **67**, 2021 (1991); E. Esarey and P. Sprangle, Phys. Rev. A **45**, 5872 (1992).
 - [13] C. B. Darrow *et al.*, Phys. Rev. Lett. **69**, 442 (1992); W. P. Leemans *et al.*, Phys. Rev. A **46**, 1091 (1992).
 - [14] T. M. Antonsen, Jr. and P. Mora, Phys. Rev. Lett. **69**, 2204 (1992); Phys. Fluids B **5**, 1440 (1993).
 - [15] J. B. Rosenzweig, B. Briezman, T. Katsouleas, and J. J. Su, Phys. Rev. A **44**, R6189 (1991).
 - [16] C. J. McKinstrie and R. Bingham, Phys. Fluids B **4**, 2626 (1992).
 - [17] A. Bers, in *Basic Plasma Physics*, edited by A. A. Galeev and R. N. Sudan, Handbook of Plasma Physics Vol. 1 (Elsevier, New York, 1983), p. 478.
 - [18] N. E. Andreev, L. M. Gorbunov, V. I. Kirsanov, A. A. Pogosova, and R. R. Ramazashvili, Pis'ma Zh. Eksp. Teor. Fiz. **55**, 551 (1992) [JETP Lett. **55**, 571 (1992)]. The major results of this work are quite similar to our own, but are limited to cases in which $|a|^2 \ll 1$.